

Seasonal Variation of Total Column Formaldehyde, Nitrogen Dioxide, and Ozone Over Various Pandora Spectrometer Sites with a Comparison of OMI and Diurnally Varying DSCOVR-EPIC Satellite Data

Jay Herman^{1,2} and Jianping Mao^{2,3}

¹GESTAR II University of Maryland Baltimore County, Baltimore, Maryland USA

1000 Hilltop Cir, Baltimore, MD 21250

²NASA Goddard Space Flight Center, 8800 Greenbelt Road, Greenbelt, MD 20771, USA

Correspondence: Jay Herman (herman@umbc.edu)

³College of Computer, Mathematical and Natural Sciences, University of Maryland, College Park, MD 20740, USA

Abstract

Both OMI (Ozone Monitoring Instrument) satellite and Pandora ground-based instruments operate with spectrometers that have similar characteristics in wavelength range and spectral resolution that enable them to retrieve total column amounts of formaldehyde TCHCHO, and nitrogen dioxide TCNO₂, and total column ozone TCO. The polar orbiting OMI observes at 13:30 ± 0:25 local time plus an occasional second side-scan point 90 minutes later at mid-latitudes. OMI has a spatial resolution of 13 x 24 km² at nadir. The ground-based Pandora spectrometer system observes the direct sun all day with a temporal resolution of 2 minutes. At most sites, Pandora data show a strong seasonal dependence for TCO and TCHCHO and less seasonal dependence for TCNO₂. However, a low pass filter Lowess fit (3-months) can reveal the seasonal dependence of TCNO₂ for both OMI and Pandora at mid-latitude sites usually correlated with seasonal heating using natural gas or oil. Compared to Pandora, OMI underestimates the amount of NO₂ air-pollution that occurs during most days, since the OMI TCNO₂ retrieval is around 13:30± 0:25 local time, which tends to occur near the frequent minimum of the daily TCNO₂ time series. Even when Pandora data is averaged between 13:00 and 14:00 hours local time OMI retrieves less TCNO₂ than Pandora over urban sites because of OMI's large field of view. The seasonal behavior of TCHCHO is mostly caused by plant growth and emissions from lakes that peak in the summer as observed by Pandora. Long-term averages show that OMI TCHCHO usually has the same seasonal dependence but differs in magnitude from the amount measured by Pandora and is frequently larger. Comparisons of OMI total column NO₂ and HCHO with Pandora daily time series show both agreement and disagreement at various sites and days. Daily time dependent comparisons of OMI TCO with those retrieved by Pandora show good agreement in most cases. Additional comparisons are shown of Pandora TCO with hourly retrievals during a day from EPIC (Earth Polychromatic Imaging Camera) spacecraft instrument orbiting the Earth-Sun Lagrange point L₁.

1.0 Introduction

Formaldehyde, HCHO, is ubiquitous in the atmosphere and as with other VOCs (Volatile Organic Compounds) are emitted from natural and anthropogenic sources, such as plants, animals, biomass burning, fossil fuel combustion, and industrial processes (Zhang et al., 2019; Morfopoulos et al., 2021). Formaldehyde is mainly produced from the oxidation of VOCs such as isoprene, methane, and anthropogenic emissions (Wittrock, 2006). Formaldehyde can also be directly emitted from some sources, such as vehicle exhaust, tobacco smoke, building materials, and wood burning affecting pollution levels both indoors and outdoors. The majority of gaseous and atmospheric formaldehyde derives from microbial and plant decomposition (Peng et al., 2022). HCHO concentrations in the first few kilometers of the atmosphere vary depending on the location, time of day, season, and meteorological conditions. Some of the factors that influence total atmospheric column amounts of HCHO are:

- **Solar radiation:** Formaldehyde is photolyzed by solar ultraviolet radiation (Nussbaumer et al., 2021), which means it is broken down into smaller molecules and radicals. The photolysis rate of formaldehyde depends on the solar zenith angle, the cloud cover, and the atmospheric composition. Generally, formaldehyde photolysis is faster during mid-day and in the summer
- **Temperature:** The thermal decomposition rate of formaldehyde increases with temperature, which means it is faster in warmer regions and seasons.
- **Humidity:** Formaldehyde reacts with water vapor in the atmosphere, forming formic acid and hydroxyl radicals. The reaction rate of formaldehyde with water vapor depends on the relative humidity, which varies with the temperature and the precipitation. Generally, formaldehyde

reaction with water vapor is faster in humid regions and seasons.

The largest sources of NO₂ are obtained from fossil fuel burning from various types of automobiles truck emissions and power generation followed by industrial processes and oil and gas production (Van der A, 2008; Stavrou et al. 2020). Additional sources are soils under natural vegetation and the oceans, agriculture and the use of nitrogen rich fertilizers, forest fires, and lightning. In populated areas requiring winter heating, anthropogenic sources of lower tropospheric NO₂ are larger than natural sources. Nitrogen oxides play a major role in atmospheric chemistry and the production and destruction of ozone in both the troposphere and stratosphere. In the boundary layer high concentrations of both HCHO (Kim et al., 2011) and NO₂ (Faustini et al., 2014) are health hazards for humans.

TCHCHO, TCNO₂ and TCO in the atmosphere are typically measured by satellite and ground-based instruments.

- Satellite: The Ozone Monitoring Instrument (OMI) is a satellite sensor launched in July 2004 that measures HCHO, NO₂, O₃, and other atmospheric constituents from space (Levelt et al. 2018). Detailed descriptions of the OMI instrument are given in Levelt et al. (2006) and Dobber et al. (2006). Briefly, OMI is a side scanning spectrometer instrument (270 to 500 nm in steps of 0.5 nm) with a nadir spatial resolution of 13 x 24 km². OMI data can be used to monitor their global distribution and long-term trends, and to investigate the role of NO₂ and HCHO in atmospheric chemistry and air quality (Lamsal et al., 2014; 2015; Boeke et al., 2011). For ozone, DSCOVR (Deep Space Climate Observatory), located at the Earth-Sun gravitational balance Lagrange point L₁, contains a filter-based instrument EPIC (Earth Polychromatic Imaging Camera) capable of obtaining TCO once per hour (90 minutes in Northern hemisphere winter) simultaneously at for the entire sunlit globe as the Earth rotates (Herman et al., 2018) with nadir resolution of 18 x 18 km². Other current satellite instruments also detect NO₂, HCHO, and O₃ such as The TROPOspheric Monitoring Instrument (TROPOMI).
- Ground-based Spectrometer: The Pandora spectrometer system forms a worldwide network of over 150 currently working direct-sun observing instruments that match atmospheric observations with known laboratory spectra of HCHO, NO₂, and O₃ to obtain the total vertical column above the Pandora instrument every 2 minutes. Pandora uses a single-grating spectrometer and a charge-coupled device (CCD) 2048 x 64-pixel detector to record the direct-sun spectra in the ultraviolet and visible wavelength range, 280 – 525 nm with an oversampled 0.6 nm spectral resolution. The retrieval algorithm is based on a spectral fitting technique to retrieve the slant column densities of O₃, HCHO, NO₂ and other gases, and then convert them to vertical column densities using geometric air mass factors appropriate for direct-sun observations. Pandora spectrometers have been deployed in various field campaigns and locations to monitor the spatial and temporal variability of TCHCHO and TCNO₂ to validate and improve the satellite observations of TCHCHO (Herman et al., 2009, Tzortziou et al., 2015, Spinei et al., 2018).

This study will examine the seasonal cycles of total column NO₂, HCHO, and O₃ seen by the Pandora instruments by examining multi-year (2021 – 2024) time series for seasonal and daily behavior at various sites and will compare with observations made from the OMI satellite overpass measurements for the Pandora sites. Pandora ozone measurements will be additionally compared to hourly data obtained from EPIC. All of the Pandora data used in this study are after the upgrade of the instruments to

eliminate internal sources of HCHO (Spinei, et al., 2021). Part of this study (TCNO₂ and TCO) is an extension of Herman et al. (2019) using Pandora data (2012 – 2017) before the internal upgrade. A difference is that Pandora TCO is now compared with hourly TCO retrieved by DSCOVR-EPIC. Table 1 shows a list of Pandora sites used in this study.

Table 1 List of 30 Pandora locations used in this study and figure of appearance					
	Pandora Number	Pandora location name	Lat (deg)	Long (deg)	Alt(m)
1	Pan 180 Fig.1	Bronx, New York USA	40.868	-73.878	31
2	Pan 64 Fig.3	New Haven, Connecticut USA	41.301	-72.903	4
3	Pan 190 Fig.4	Bangkok, Indonesia	13.785	100.540	6
4	Pan 182 Fig.5	Tel Aviv, Israel	32.113	34.806	8
5	Pan 159 Fig. 6	Wakkerstroom, South Africa	-27.349	30.144	18
6	Pan 20 Fig.7	Busan, Korea	50.798	4.358	107
7	Pan 145 Fig.10	Toronto-Scarborough, Canada	43.784	-79.187	14
8	Pan 134 Fig. 12	Bristol, Pa, USA	40.107	-74.882	10
9	Pan 204 Fig. 12	Boulder, Co USA	40.038	-105.242	161
10	Pan 106 Fig.12	Innsbruck, Austria	47.264	11.385	616
11	Pan 117 Fig.12	Rome Italy	41.907	12.5158	75
12	Pan 193 Fig.12	Tsukuba, Japan	36.066	140.124	51
13	Pan 140 Fig.13	Washington, DC USA	38.922	-77.012	6
14	Pan 166 Fig.7	Philadelphia, Pa USA	39.992	-75.081	6
15	Pan 238 Fig.14	Granada	37.164	-3.605	7
16	Pan 240 Fig. 14	Thessaloniki, Greece	40.6336	22.9561	60
17	Pan 66 Fig.15	Huntsville Alabama USA	34.725	-86.646	22
18	Pan 156 Fig.15	Hampton, Virginia USA	37.020	-76.337	19
19	Pan 39 Figs.12,15	Dearborn, Michigan USA	42.307	-83.149	18
20	Pan 101 Fig.A1	Izania, Spain	28.309	-16.499	24
21	Pan 119 Fig.A1	Athens, Greece	37.998	23.775	130
22	Pan 124 Fig.A1	Comodoro Rivadavia	-45.7833	-67.45	46
23	Pan 131 Fig. A1	Palau	7.3420	134.4722	23
24	Pan 135 Fig.A1	CCNY Manhattan NY USA	40.815	-73.951	34
25	Pan 142 Fig.A1	Mexico City, Mexico	19.326	-99.176	2280
26	Pan 146 Fig.A1	Yokosuka, Japan	35.321	139.651	5
27	Pan 147 Fig.A1	Detroit, Mi USA	42.303	-83.107	178
28	Pan 150 Fig.A1	Ulsan, Korea	35.575	129.190	38
29	Pan 154 Fig.A1	Salt Lake City Ut, USA	40.766	-75,081	1455
30	Pan 162 Fig.A1	Brussels, Belgium	50.798	4.358	107

2.0 Examples of Seasonal and Daily Variation of HCHO and NO₂

Worldwide Pandora total column data can be downloaded from the Austrian Pandonia project website <https://data.pandonia-global-network.org/> or from a US NASA backup site updated every week. https://avdc.gsfc.nasa.gov/pub/DSCOVR/Pandora/DATA_02/. Of interest for this study are the Level-2 (L2) time series ASCII files for direct-sun observations. For example, the Bronx New York City files for Pandora instrument 180 for TCNO₂ data are in Pandora180s1_BronxNY_L2_rnvs3p1-8.txt, TCHCHO in Pandora180s1_BronxNY_L2_rfus5p1-8.txt, and TCO data in Pandora180s1_BronxNY_L2_rout2p1-8.txt with the 9 bold characters identifying the file contents.

The Pandora data are arranged in irregular columns that are identified in the metadata header for each file. In the current version, column 1 contains the GMT date and time for each measurement and column 39 contains measured column density in moles m^{-2} (multiply by $6.02214076 \times 10^{23} / 2.6867 \times 10^{20} = 2241.4638$ to convert to DU where $1 \text{ DU} = 2.6867 \times 10^{20} \text{ molecules m}^{-2}$). Pandora data also contain measurements of water vapor, and SO_2 total column amounts.

The original OMI data has a resolution of $13 \times 24 \text{ km}^2$ at the center of the OMI side-to-side scan. The overpass OMI data is based on the latest gridded version with $0.25^\circ \times 0.25^\circ$ pixel resolution. The closest OMI pixel to each Pandora site within 50 km is used for the time matched comparison. Long term time series use all available Pandora data between 07:00 and 17:00. Diurnal comparisons with OMI on specified days use Pandora minute-by-minute data that are nearly continuous suggesting that Pandora is observing the direct sun under clear sky conditions.

Figure 1 shows the seasonal and daily variation of total column HCHO (TCHCHO) and NO_2 (TCNO2) using all of the Pandora data between 07:00 and 17:00 obtained during each day in Bronx, New York filtered by the estimated RMS error being less than the total column value. The daily data for 1 week in July and September shows the range of values for both weekdays and weekends. When all the Bronx TCHCHO data are plotted as an aggregate for 3 years, there is a strong seasonal pattern with a maximum in July and a minimum near the end of December. The summer seasonal dependence of TCHCO is consistent with the surface HCHO values observed by the ground-based Air-Quality System AQS (Wang et al., 2022). For TCNO2, there is a weaker seasonal pattern as shown in the Lowess(0.033) fit to the data (Cleveland, 1979; Cleveland and Devlin, 1988) with moderate maxima in January-February, since the sources of NO_2 are largely from the nearly constant flow of cars and trucks. The parameter 0.033 is the fraction of the time-series data included in the local least squares estimate, or about 1 month.

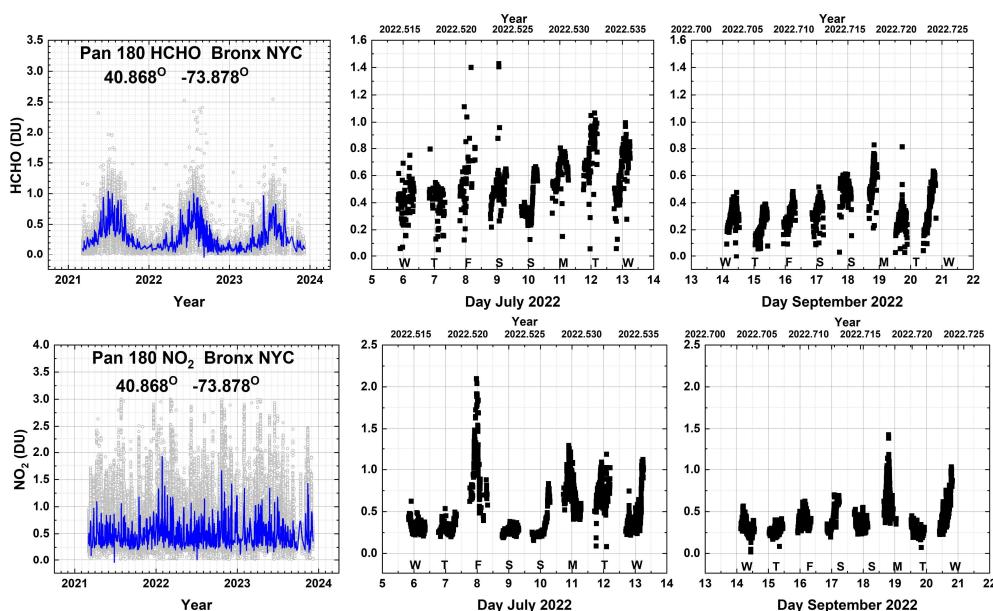


Fig. 01 Seasonal and daily behavior of HCHO and NO_2 from Pan 180 located in the Bronx, NYC at 40.868°N , -73.878°W . The blue lines are a Lowess(0.033) fit to the data (light grey), which is approximately a 1-month local least-squares average. The Local principal investigator for Pan 180 is Dr. Luke Valin.

Figure 2 shows the daily average of Pandora data obtained from diurnal variation of TCHCHO and TCNO₂ from 09:00 to 15:00 local standard time (GMT – 5). The primary emission sources of atmospheric HCHO include direct emission from vegetation, the soil, biomass burning, and decaying plant and animal matter. This is consistent with the Bronx location that is adjacent to a large, vegetated park with a small lake near Fordham University. The same TCHCHO seasonal dependence and magnitude occurs when the Pandora sampling is restricted to 13:00 to 14:00 local standard time similar to the OMI overpass time.

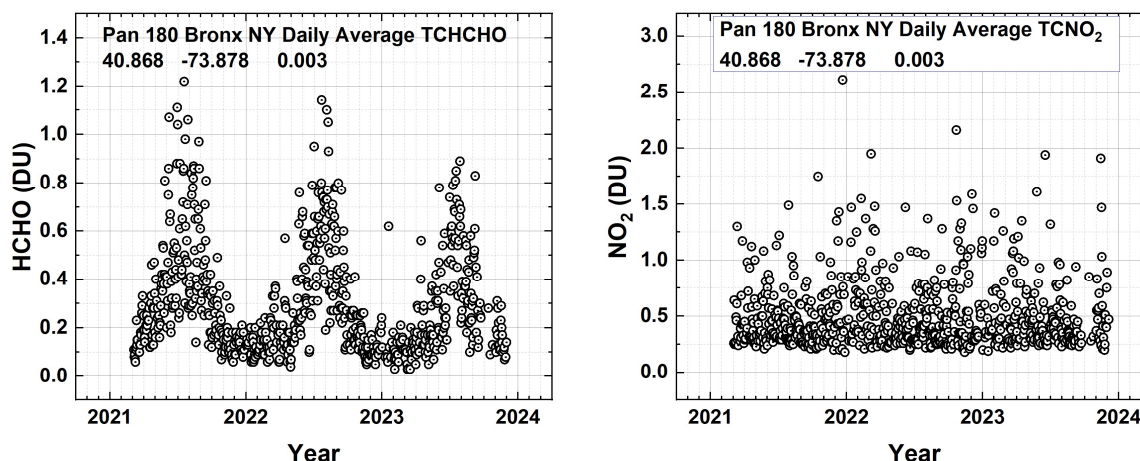


Fig. 02 The daily average seasonal variation of HCHO and NO₂ over Fordham University in Bronx, New York City from Pandora 180 at 40.868° latitude, -73.878° longitude, and 0.003 km altitude. Each point is a daily average of the data in Fig.1. Local principal investigator: Dr. Luke Valin

There are 3 Pandora sites in New York City and one in nearby Bayonne, New Jersey. The NYC sites are in the Bronx-Fordham University, Manhattan-City College NY (CCNY), Queens-Queens College. All four successfully measured NO₂ in the period 2021 – 2023. A strong seasonal cycle in TCNO₂ is not seen (Figs. 1 and 2) in the traffic driven production of NO₂ in the Bronx, New York. The mean values of total column NO₂ (TCNO₂) for each of the 3 New York sites are 0.5 DU while the TCNO₂ for the port city of Bayonne, NJ is substantially higher at 0.7 DU. None of the four sites show a large seasonal daily average TCNO₂ pattern. For TCHCHO, all four sites show an annual seasonal cycle with three of the sites having a 3-year average of 0.3 DU except for the Queens site at 0.45 DU. The Queens site may be anomalous because of many missing points affecting the average.

Similar behavior is seen at other sites such as the one from New Haven Connecticut located in a vegetated area adjacent to two rivers (Fig.3). TCHCHO has a clear summer peak in June – July and a weak winter TCNO₂ peak in December to January coinciding with the maximum heating season.

The seasonal variation of TCHCHO could not be studied prior to the internal upgrade of Pandora after 2019 that was needed because of the release of HCHO from polyoxymethylene (POM-H Delrin) out-gassing as a function of daytime temperature within the Pandora sun-pointing head (Spinei et al., 2021)

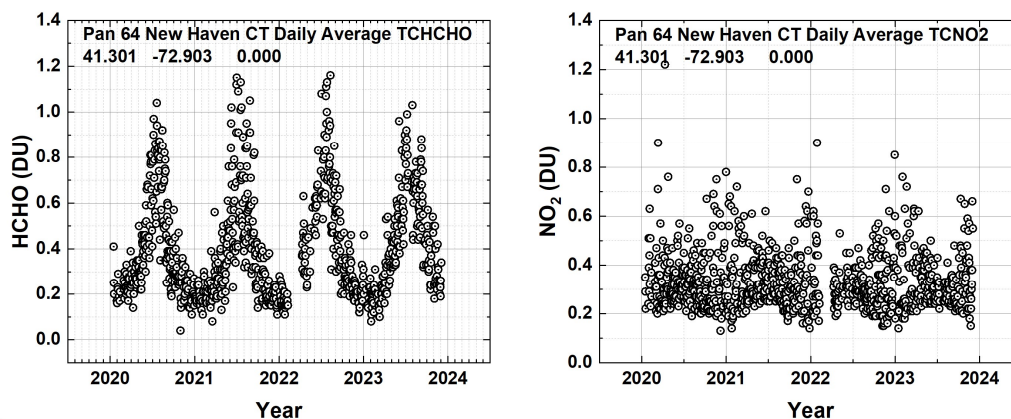


Fig. 03 The seasonal variation of TCHCHO and TCNO2 over New Haven Connecticut from Pandora 64 at 41.301°N latitude and -72.903°W longitude. Each point is a daily average. Local principal investigator: Dr. Nader Abuhassan

177
 178 An equatorial Pandora site (Fig. 4) with a sufficiently long data record is located in Bangkok, Indonesia
 179 near a small park and lake. Bangkok has a tropical monsoon climate with three main seasons: hot season
 180 from March to June, rainy season from July to October, and cool season between November and
 181 February. TCHCHO has a seasonal cycle peaking in March – April when the sun is nearly overhead and a
 182 minimum during the rainy season. TCNO2 has a clear seasonal cycle peaking in December – January and
 183 a minimum during the rainy season. Bangkok has a tropical climate with April as the hottest month with
 184 temperatures averaging at 30.5°C (87°F) and the coldest is December at 26°C (79°F).

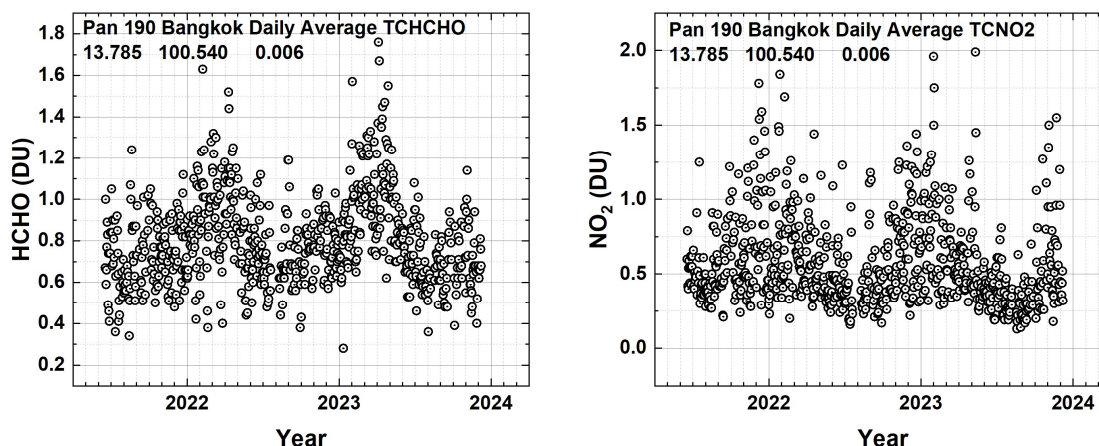


Fig. 04 The seasonal variation of TCHCHO and TCNO2 over equatorial Bangkok Indonesia at 13.785°N and 100.540°E . The local principal investigator is Surassawadee Phoompanit.

185
 186 An unusual counter example to the typical TCHCHO seasonal cycle is for the Pandora site located in Tel
 187 Aviv Israel. Tel Aviv has significant amounts of HCHO but does not show seasonal variation in TCHCHO
 188 because of a coastal location in a warm climate even at midlatitudes located at 32.113°N , 34.085°E that
 189 has essentially two seasons, a cool, rainy winter: October – April and a dry, hot summer: May –
 190 September. The result is there is limited seasonal increase in vegetational activity and almost no
 191 seasonal variation in HCHO (Fig. 5). However, TCNO2 shows a clear seasonal increase in the December -

January months frequently reaching over 0.5DU. The TCNO₂ seasonality is similar to that of the near-surface concentrations reported by Boersma et al., (2009). The Pandora instrument 182 is located at Tel Aviv University about 1 km from a major highway. Tel Aviv has frequent episodes of smog associated with heavy automobile and truck traffic (Newmark, 2001). Heating and cooling in Tel Aviv are mainly electrical with the maximum power generation occurring in the summer, suggesting that the winter TCNO₂ peak is not caused just by electrical power generation from natural gas that emits NO₂.

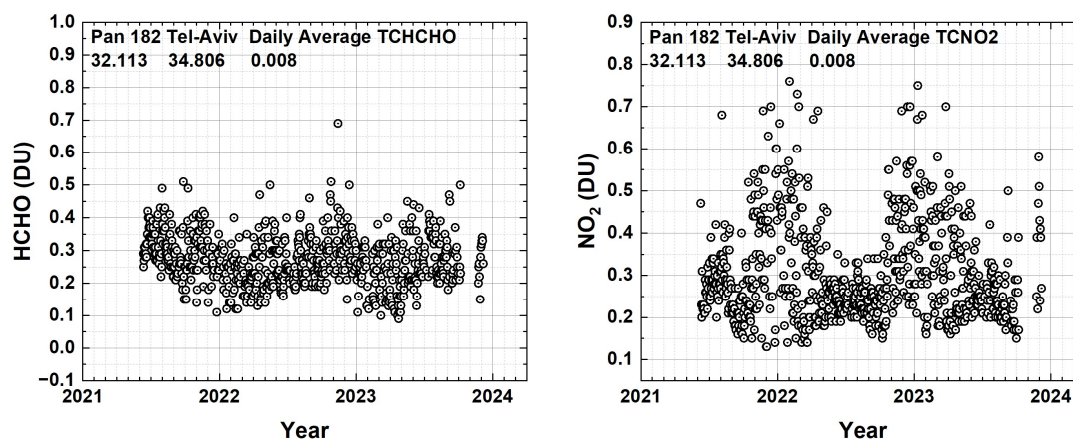


Fig. 05 Seasonal variation in daily average TCHCHO and TCNO₂ in Tel Aviv Israel from Pandora 182 located at 32.113°N, 34.085°E at a height of 8 meters. The local principal investigator for Pan 182 is Dr. Michal Rozenhaimer.

Finally, a Pandora example from the Southern Hemisphere SH from Wakkerstroom, South Africa located in a rural area near the ocean a few degrees outside of the equatorial zone at -27.359°S and 30.144°E.

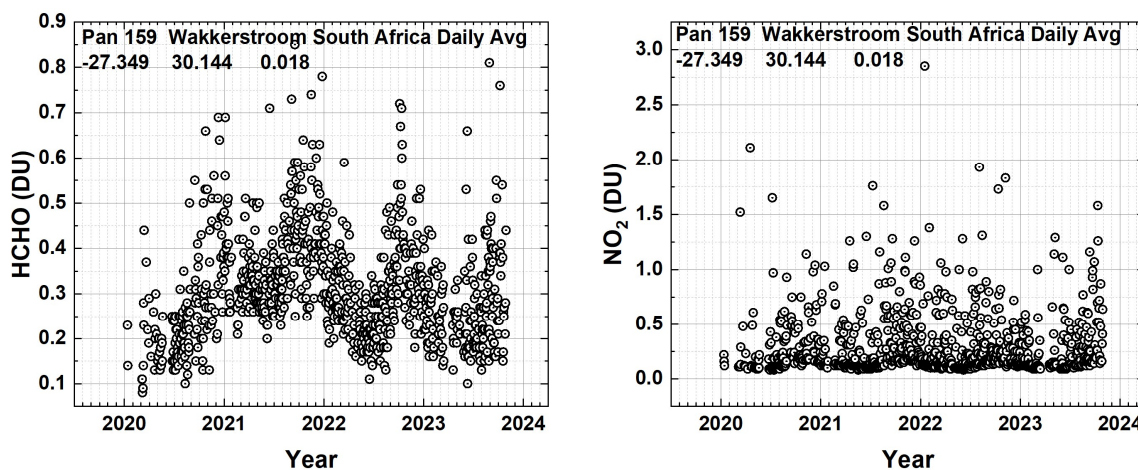


Fig. 06 Seasonal variation in daily average HCHO and NO₂ in Wakkerstroom South Africa from Pandora 159 located at -27.359°S and 30.144°E at a height of 18 m. Local principal investigator: B. Scholes

As expected, the peak value of TCHCHO occurs near the SH summer in November – December, while TCNO₂ has no significant seasonal dependence.

2.1 Comparisons Between Pandora and OMI Retrievals of NO₂ and HCHO

In this section three types of comparisons of Pandora with OMI satellite data are considered. First (Fig. 7 upper panels), is the TCNO₂ time series consisting of the data record of Pandora and OMI from 2020 – 2023. The second (Fig. 7 lower panels) is a low-pass Lowess(3-months) filter of midday TCNO₂ showing the seasonal variation. The third (Fig. 8), looks at a few selected days in May, July, and December and compares Pandora values with the mid-afternoon OMI overpass at times near 13:30 hours equator crossing time. Pandora and OMI data are matched at the same GMT and then converted to local solar time, GMT + Longitude/15. The OMI overpass HCHO and NO₂ data are found at <https://avdc.gsfc.nasa.gov/pub/data/satellite/Aura/OMI/V03/L2OVP/OMHCHO/>.

<https://avdc.gsfc.nasa.gov/pub/data/satellite/Aura/OMI/V03/L2OVP/OMNO2/>.

Figure 7 (upper 2 panels) illustrates that OMI only captures a fraction of the daily values of total column NO₂ and fails to detect the extent of the daily pollution at both the Bronx New York City and Busan Korea sites. This is because OMI and other polar orbiting satellites only collect data once per day (occasionally twice per day) at any given location at mid-afternoon, frequently when TCNO₂ is below its daily maximum (Herman et al., 2019; Lamsal et al., 2015). The lower 4 panels of Fig. 7 reveal the seasonal dependence of TCNO₂ at two mid-latitude Northern Hemisphere sites found by using a 3-month low-pass filter Lowess(3 Months) showing that there is an annual TCNO₂ cycle peaking in the winter that corresponds to the natural gas and oil heating use. OMI and Pandora TCNO₂ agree more closely when the comparison is restricted to the overpass time. The Pandora (13:00 to 14:00) values are larger than those from OMI especially at Busan suggesting that the OMI gridded overpass field of view 0.25° x 0.25° includes areas of lower NO₂ values over the nearby ocean. In the case of the Bronx, the differences are smaller but also include areas over rivers. Philadelphia Pennsylvania is landlocked but smaller than an OMI gridded footprint so that the OMI field of view contains somewhat less polluted suburbs making the OMI TCNO₂ closer to the Pandora values. The Boulder Colorado Pandora is in a small landlocked city where the OMI field of view extends over sparsely populated regions leading to OMI TCNO₂ lower than Pandora values.

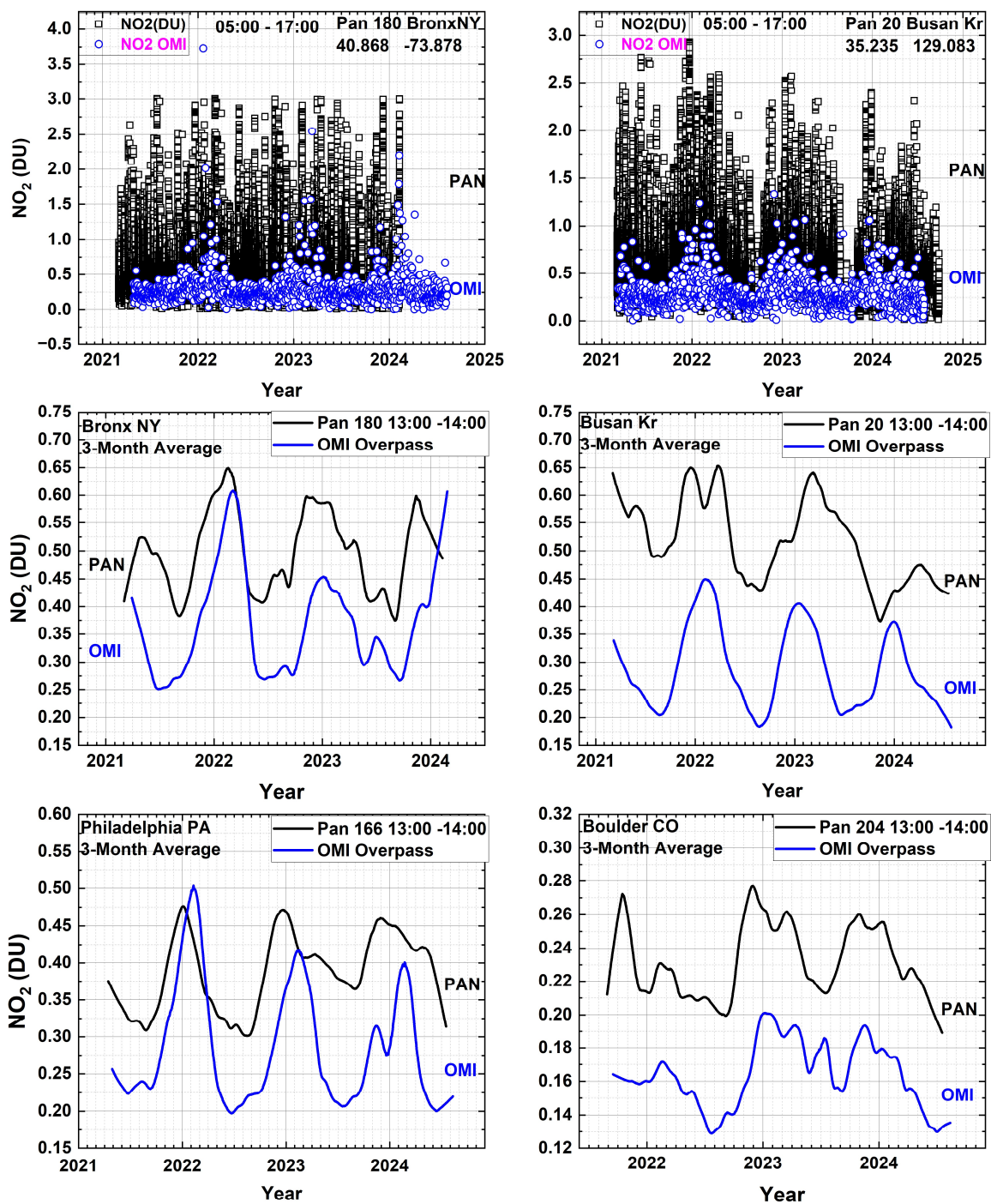


Fig. 07 Upper 2 Panels: Comparison of OMI (approximately 13:30) and Pandora (07:00 – 17:00) total column NO₂ time series in Bronx NY (40.868°N, -73.878°W) and Busan Korea (35.235°N, 129.083°E). Lower 4 Panels: Pandora data for Bronx, Busan, Philadelphia (39.992°N, -75.081°W) and Boulder (40.0375°N, -105.242°W) are averaged between 13:00 – 14:00 hours. Both OMI (blue) and Pandora (black) then have a Lowess(3-month) low-pass filter applied. Local principal investigator for Pan20 is Jae Hwan Kim, for Pan 180 and Pan 166 is Dr. Luke Valin, and for Pan 204 Dr. Nader Abuhassan.

Figures 8 and 9 show the diurnal daytime variation for 3 selected days for Pandora retrieved total column NO_2 and HCHO compared with OMI at the overpass time for both the Bronx in New York City, Busan, Korea and Philadelphia, Pennsylvania. These are typical examples of the highly variable hourly variation of TCHCHO and TCNO₂ as observed by Pandora at most sites.

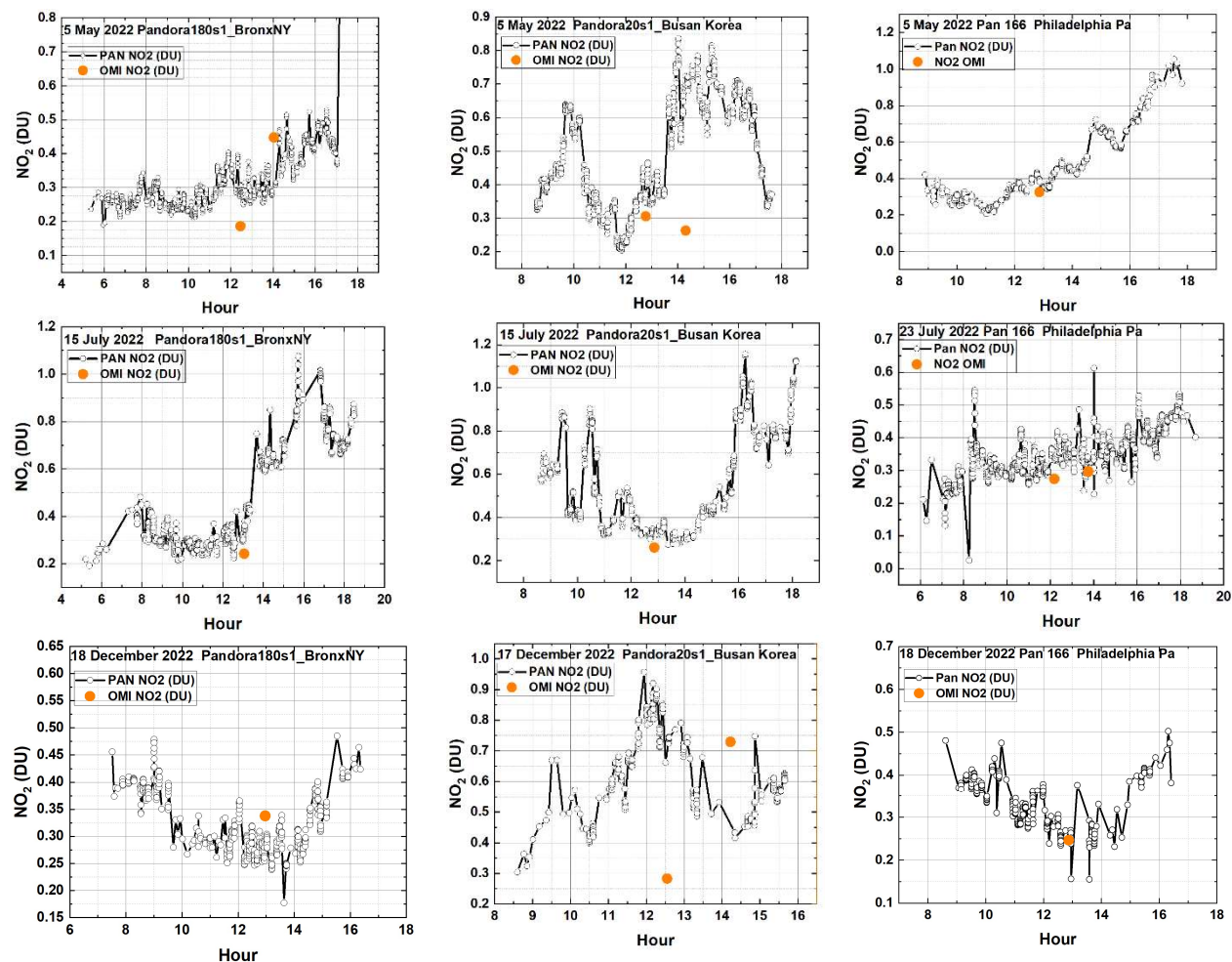


Fig. 08 A comparison between Pandora and OMI (Orange circle) total column NO_2 for 3 locations (Bronx, New York, Busan Korea, Philadelphia, Pennsylvania). The Local principal investigator for Pan 180 and Pan 166 is Dr. Lukas Valin and for Pan 20 is Dr. Jae Hwan Kim.

The hourly variation of TCHCHO and TCNO₂ on any given day can take on unique shapes depending on the presence of surface winds, changes in temperature, and sunlight. The variability of TCNO₂ is also driven by the strength of the sources (automobile exhaust, power generation, industry, etc.) as well as the meteorological conditions. Occasionally, there is good agreement (within 10%) but in general the OMI overpass values do not agree with Pandora retrieved values for both TCHCHO and TCNO₂. In the sample shown in Figures 8 and 9, the cases of agreement are about 70% of the time for TCNO₂ and 30% for TCHCHO.

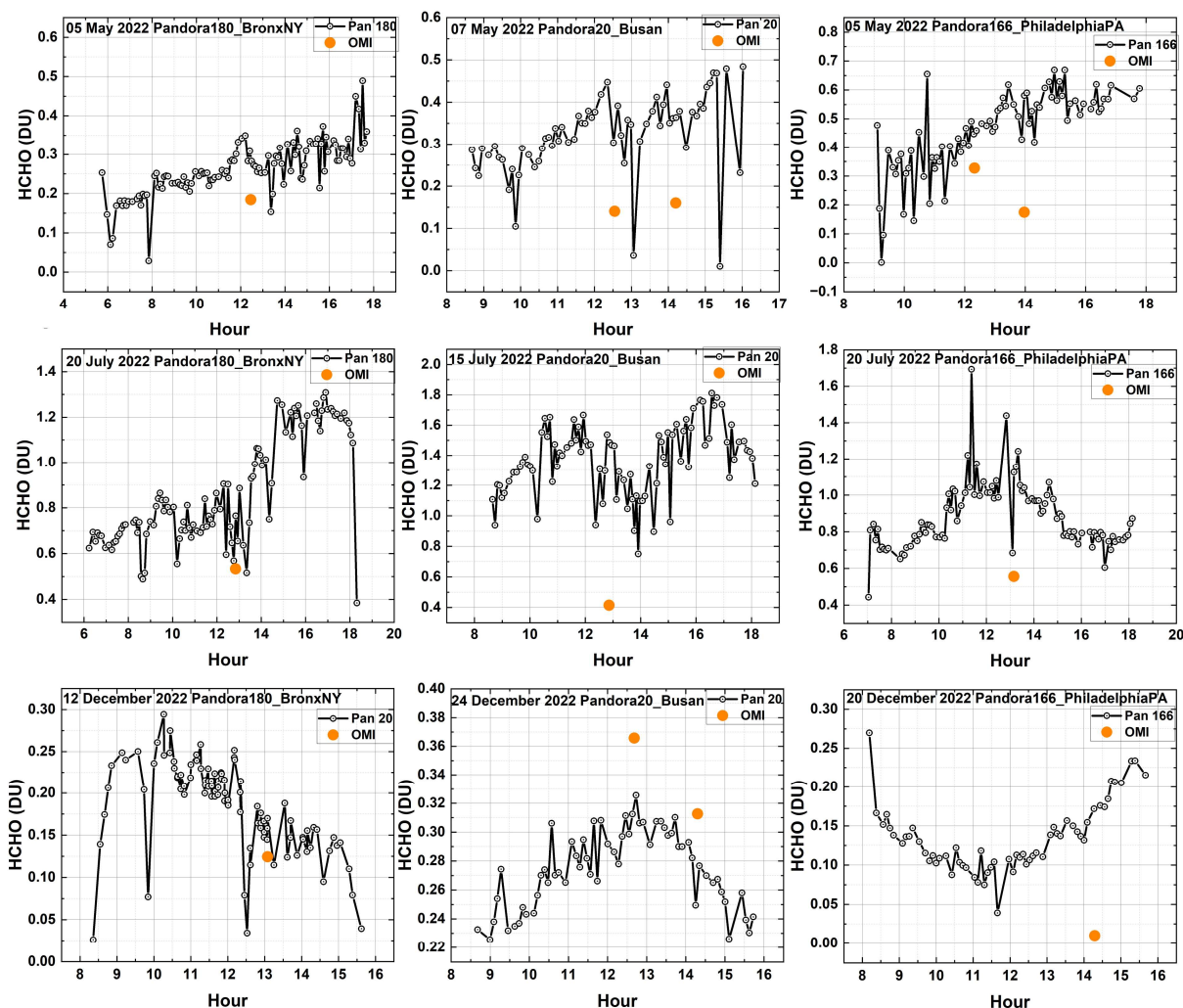


Fig. 09 A comparison between Pandora and OMI (orange circle) total column HCHO. The Local principal investigator for Pan 180 and Pan 166 is Dr. Luke Valin and for Pan 20 is Dr. Jae Hwan Kim.

249

250 Figure 9 illustrates the comparison of TCHCHO retrievals from Pandora and OMI. The spectral fitting
 251 algorithm for detecting HCHO absorption is in the same short wavelength UV spectral region as used for
 252 ozone retrieval, 300 – 360 nm (Gratien et al. 2007). This means that the retrieval sensitivity for “seeing”
 253 all the way to the surface is reduced because of ozone absorption and Rayleigh scattering. Also, small
 254 errors in ozone retrieval can affect the detection of HCHO. This problem is not present for the spectral
 255 fitting of NO₂, since that usually occurs in the visible range 410 – 450 nm where there is only
 256 interference from a weak and narrow water vapor line.

257 Pandora TCHCHO daily average data (Fig. 10) for University of Toronto in Toronto-Scarborough (Lat =
 258 43.784°N, Lon = -79.187°W) shows clear peaks in the summer from the vegetation in a surrounding park
 259 area whereas TCNO₂ shows only small seasonal variation with small peaks also occurring in the summer
 260 for values less than 0.4 DU. Higher values do not show any seasonal variation. The University of Toronto
 261 is located near a major highway, which is a strong source of NO₂ from automobiles and trucks. Unlike
 262 many sites, OMI TCHCHO data over Toronto East (centered on 43.74°N, -79.27°E is about 8 km from the

263 Pandora site) also shows sporadic summer peak values that are higher than the Pandora 13:00-14:00
 264 averages and all of the Pandora data (Fig. 11).

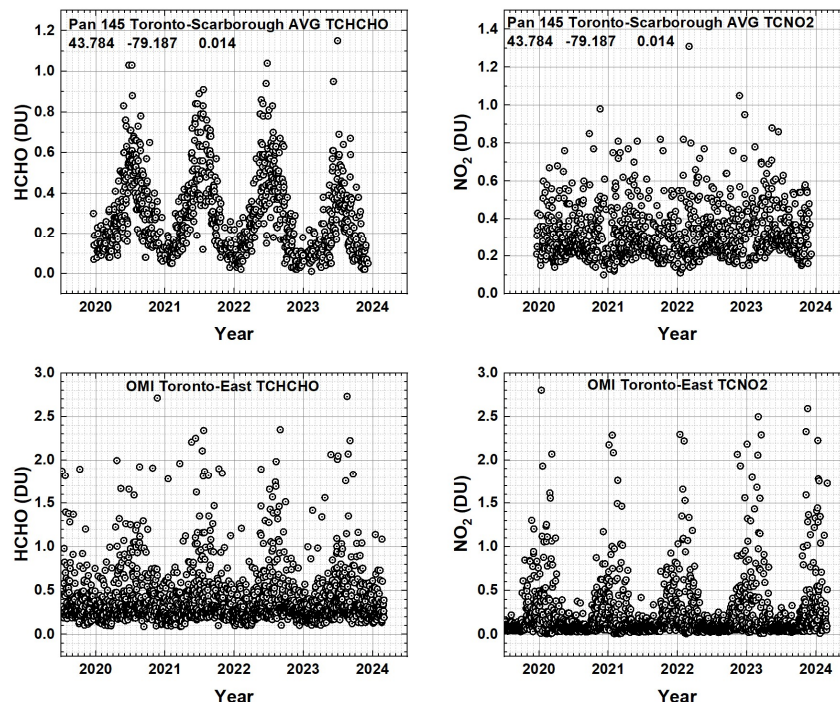


Fig. 10 A comparison of Pandora TCHCHO and TCNO2 daily average total column amounts for Toronto-Scarborough University of Toronto and OMI data for Toronto East (43.740°N, -79.270°W at approximately 13:20±0:20 Local Sun Time, GMT + Longitude/15). The local principal investigator for Pan 145 is Dr. Vitali Fioletov.

265
 266 Using the daily average Pandora data over Toronto-Scarborough (Fig. 10 upper right) shows no visible
 267 hint of an TCNO2 annual cycle that peaks in winter while the OMI TCNO2 amounts at 13:40 show a clear
 268 peak in December – January corresponding to the peak winter heating for the city (Figs. 10 lower right).
 269 Instead of the daily average data, using the average TCNO2 from 13:00 to 14:00 to correspond to the
 270 OMI overpass time and then applying a Lowess(3 month) low-pass filter (Fig. 11) shows less TCNO2 and a
 271 weaker annual cycle that corresponds to the annual cycle observed by OMI. The OMI FOV includes the
 272 city of Toronto.

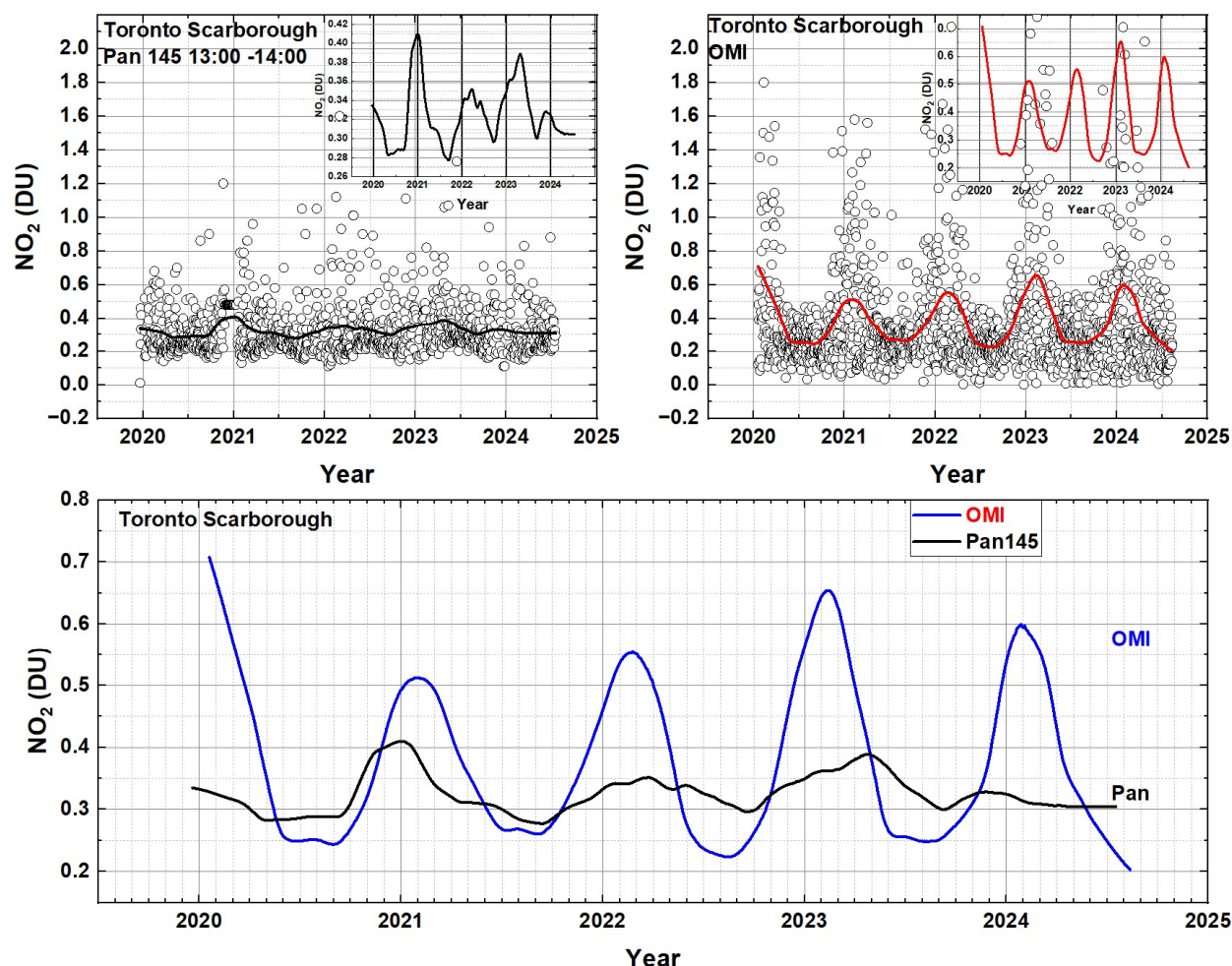


Fig. 11 TCNO₂ annual cycle for Toronto Scarborough from Pan 145 average between 13:00 and 14:00 and OMI. The smooth curves are Lowess(6 Months).

273

274 The lower panel in Fig. 11 reproduces the inset values showing the OMI has a stronger TCNO₂ annual

275 cycle because it includes the city area of Toronto. Pandora 145 picks up a small amount of the seasonal

276 signal from Toronto.

277 As shown in Fig. 12, the TCHCHO low-pass filtered time series (2021 – 2024), Lowess(3-months),

278 measured by OMI and Pandora frequently do not agree. An example is the comparison over Bronx, NY

279 (Lat = 40.868° Lon = -73.878°) where the Pandora 180 is located in a park with a small lake, while OMI

280 gridded data is averaged over a large area 33 x 33 km² in New York City with little vegetation.

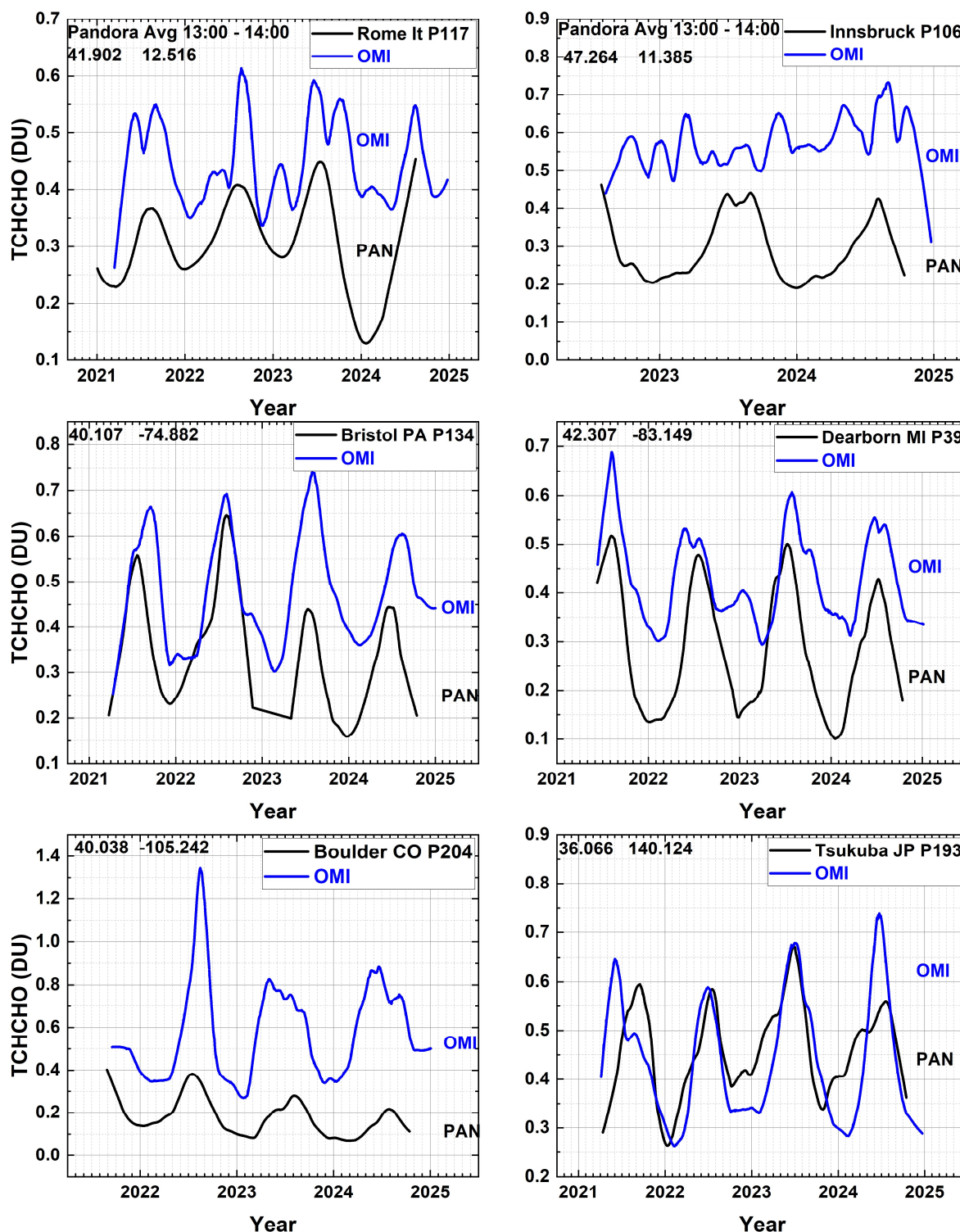


Fig. 12 A comparison between low-pass filtered, Lowess(3 months), OMI and Pandora at six sites with varying degrees of agreement with $TCHCHO(Pan) < TCHCHO(OMI)$. The Local Principal Investigators are P106 Dr. Stefano Casadio, Dr. Kei Shiomi P193, Dr. Alexander Cede P204, Dr. Lukas Valin P39; P134, and Dr. Martin Tiefengraber P106. Latitudes and longitudes are in each upper left corner.

The disagreement over Boulder Colorado may be caused by OMI's large field of view that includes lower altitude grasslands. Except for a few cases (e.g., Bronx, NY) OMI and Pandora see the same annual cycle.

2.2 Total Ozone Column

The retrieval of total column ozone amounts TCO (Figs. 13) serves as a check on the calibration of both OMI and Pandora that is also needed for spectrally overlapping TCHCHO retrievals. Comparisons of Pandora TCO with TCO measured by OMI show good agreement suggesting both instruments are well calibrated in the UV range also needed for retrieving TCHCHO. The good TCO agreement is partly because most of the O_3 is in the stratosphere near 25 km and the fact that ozone is slowly changing spatially over the OMI field of regard for the overpass data. Figure 13 shows an example obtained over Washington DC from the roof of the NASA Headquarters building and from the roof of a building at Pusan University, Korea. Other sites show similar good monthly average agreement.

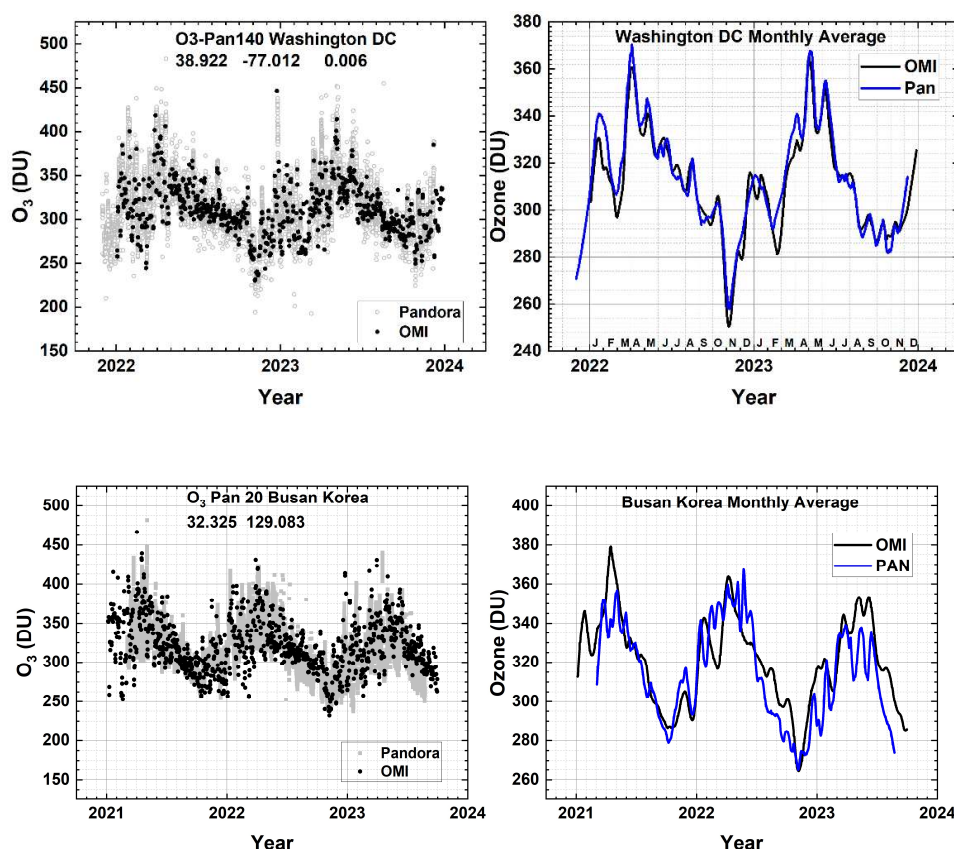


Fig. 13 A comparison of OMI Total Column Ozone values with those obtained from Pandora 140 over the Washington DC site at 38.922°N and -77.012°W and with those obtained from Pandora 20 over the Busan, Korea site at 32.325°N and 129.083°E . The smooth curves (right panel) are Lowess(6-month) fits to data in the left panel. The local principal investigator for Pan 140 is Dr. Jim Szykman and for Pan20 is Jae Hwan Kim.

294 A test of Pandora UV data is a comparison between EPIC, OMI and Pandora TCO at the specific OMI and
 295 EPIC overpass times (Fig. 14 and 15). that shows good agreement within 1 to 3 %. OMI TCO overpass
 296 data for all Pandora sites and more are available from

297 <https://avdc.gsfc.nasa.gov/pub/data/satellite/Aura/OMI/V03/L2OVP/OMTO3/>

298 There is also good agreement between daily OMI TCO with that obtained from Pandora (Fig. 14) at most
 299 sites. The values obtained at Granada differ by about 8 DU or 2.9 %.

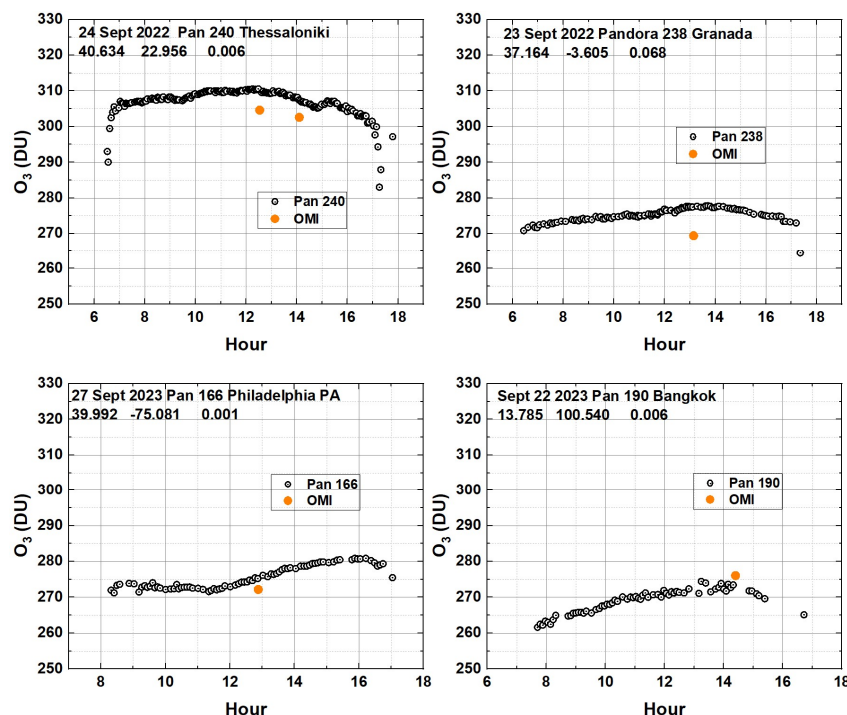


Fig. 14 A comparison of Pandora and OMI retrievals of total column O_3 at the time of the OMI satellite overpass. Local Principal Investigators: Pan 240 Alexander Cede, Pan 238 Inmaculada Foyo Moreno, Pan 166 Lukas Valin, and Pan 190 Surassawadee Phoompan.

The diurnal variation of TCO seen by Pandora can be compared (Fig. 15) with that observed by the Earth Polychromatic Imaging Camera (EPIC) on the DSCOVR (Deep Space Climate Observatory) satellite orbiting about the Earth-Sun gravitational balance Lagrange-1 point (Herman et al., 2018). EPIC obtains simultaneous data from sunrise to sunset once per hour (once per 90 minutes during Northern Hemisphere winter) as the Earth rotates in EPIC's FOV (field of view). Examples of EPIC's view of the whole illuminated Earth are available from <https://epic.gsfc.nasa.gov/>. The spatial resolution for TCO is $18 \times 18 \text{ km}^2$ at the center of the image (the color images have $10 \times 10 \text{ km}^2$ resolution). Retrievals earlier than 07:00 and after 17:00 are not reliable for EPIC or Pandora because of high solar zenith angle effects (spherical geometry effects for $\text{SZA} > 75^\circ$) not included in the retrieval algorithms. In the case of EPIC, this is compounded by high View Zenith Angles VZA outside of 07:00 to 17:00 local sun time.

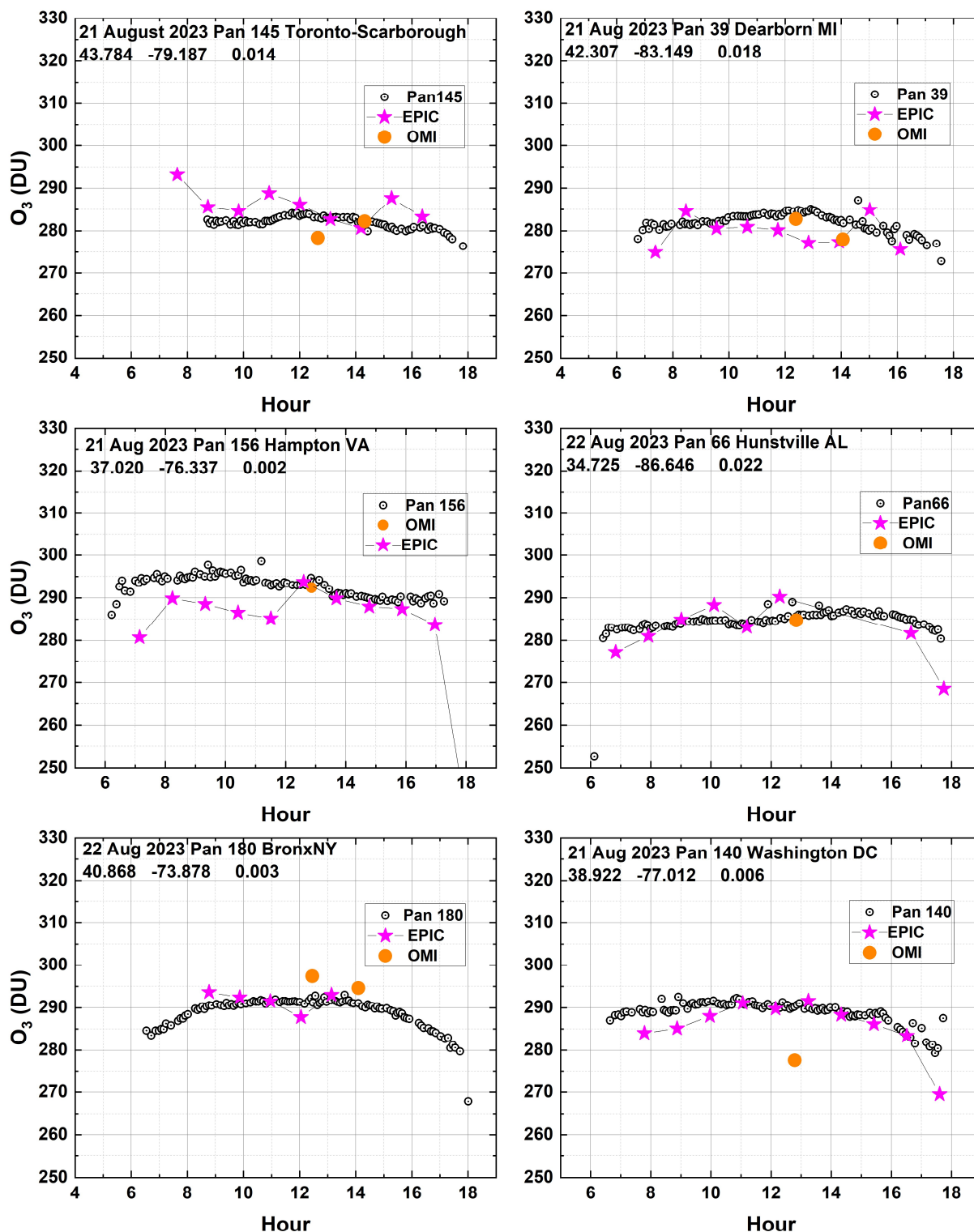


Fig. 15 A comparison of Pandora (Open Circles), EPIC (magenta stars), and OMI (orange circles) retrievals of total column O_3 at the times of the satellite overpasses. Local Principal Investigators: Pan 145 Vitali Fioletov, Pan 66 Lukas Valin, Pan 39 Lukas Valin, Pan 156 Alexander Cede, Pan 66 Nader Abuhassan, Pan180 Lukas Valin, and Pan 140 Jim Szykman

For the cases shown, the TCO data are properly retrieved between 07:00 and 17:00 local solar time. The 10:20 and 11:30 EPIC value for Hampton, VA of 286.5 and 285DU differs from Pandora by -3 %. Other differences are smaller. Occasionally, OMI differs from Pandora values as is the case, -4.6 %, for 21 August 2023 over Washington, DC.

3.0 Summary

Typical examples of the seasonal variability of HCHO, NO₂, and O₃ in terms of their measured total column TCHCHO, TCNO₂, and TCO have been presented from both Pandora Spectrometer instruments and the OMI spectrometer instrument overpass retrievals for selected Pandora sites. For most sites, OMI observes the strong seasonal variation of TCHCHO that is also clearly seen in the Pandora data and in surface measurements (Wang et al., 2022). OMI TCHCHO retrievals are usually larger than those retrieved by Pandora but not always (Fig. A2). The amount of seasonal variation for TCHCHO varies depending on the site. For most midlatitude sites, the seasonal variation is significant with peak values occurring during the summer.

OMI TCNO₂ at one shown site, Toronto-Scarborough, appears to show seasonal variability that the Pandora 145 does not appear to see. However, limiting the data to the OMI overpass time between 13:00 and 14:00 and applying a Lowess(3-months) low-pass filter reveals a weak annual cycle compared to OMI. This could be because OMI is detecting the NO₂ source from winter heating in the city, while the Pandora site (University of Toronto campus) is fairly remote from Toronto city buildings and is mostly affected by road traffic as the source of NO₂. The same low-pass filter technique applied to other sites (e.g., Bronx, NY, Busan, Korea, Philadelphia, Pennsylvania, and Boulder, Colorado) also show an annual cycle corresponding to winter heating based on combustion.

A comparison between the multi-year time series of Pandora and OMI TCNO₂ in urban areas shows that OMI is underestimating the degree of atmospheric NO₂ pollution. The results for TCNO₂ and TCO agree with data, 2012 – 2017, from a previous study before the Pandora upgrade (Herman et al., 2019). When Pandora is limited to an average of data obtained between 13:00 and 14:00 hours, the agreement between Pandora and OMI TCNO₂ is better. Comparisons of Pandora daily time series of TCHCHO and TCNO₂ with OMI overpass values show agreement about 50 % of the time.

Total column ozone agrees well in both seasonal variation and in the comparison with Pandora at the OMI overpass time. Given the nature of the ozone retrieval algorithm, the good agreement with TCO suggests that the UV calibrations for both Pandora and OMI are correct. At most well-calibrated Pandora sites, there is good agreement between Pandora TCO with the hourly TCO obtained from the DSCOVR-EPIC instrument observing the Earth from an orbit about the Earth-Sun gravitational balance Lagrange-1 point.

339 Appendix

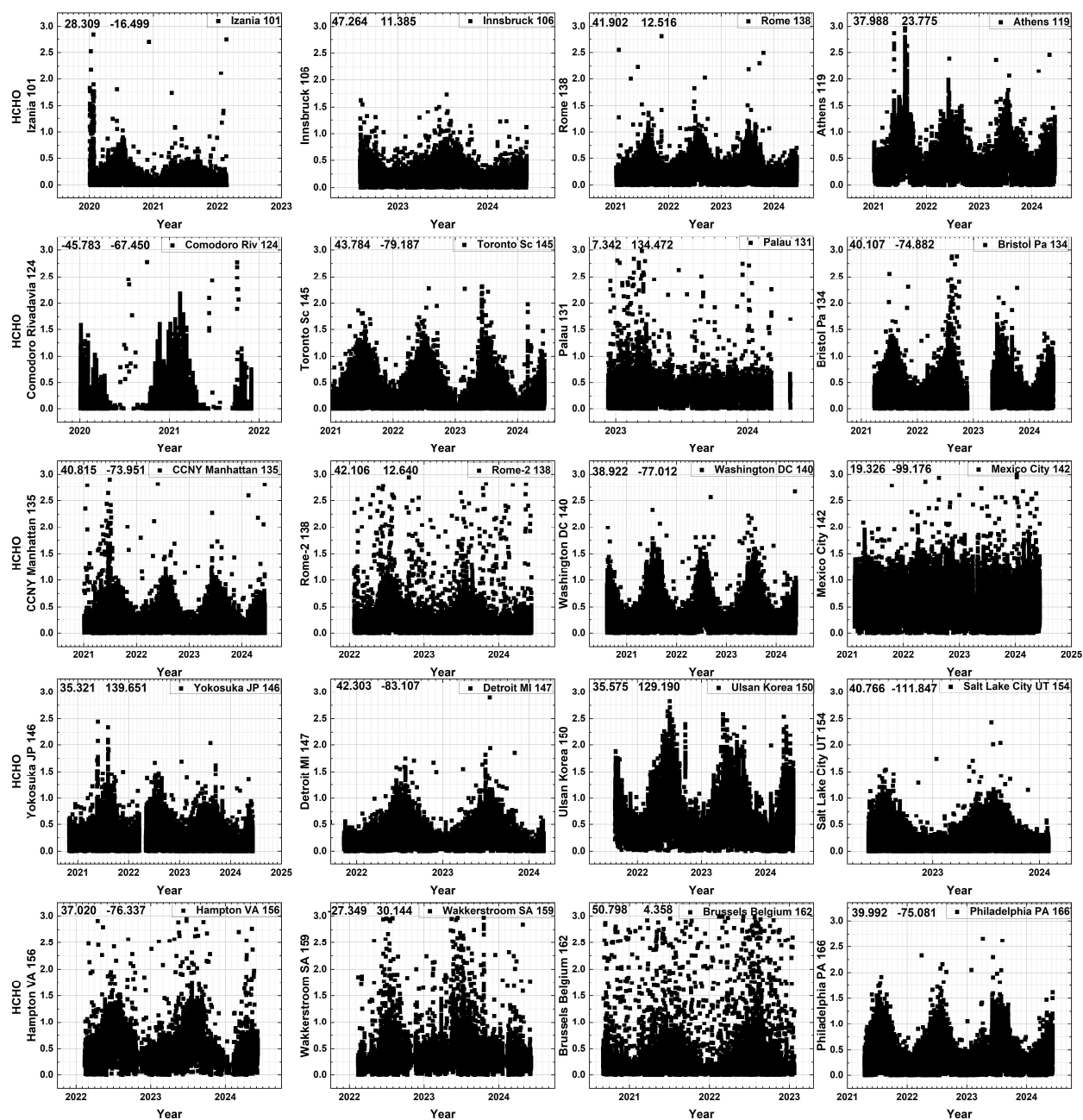


Fig. A1 The seasonal cycle of TCHCHO in DU from 20 randomly selected Pandora TCHCHO time series. The numbers in the upper left corner are the latitude and longitude in degrees and the Pandora instrument number in the right corner.

340

341 Figure A1 shows the seasonal dependence of TCHCHO with the majority of sites showing a maximum
 342 TCHCHO in mid-summer.

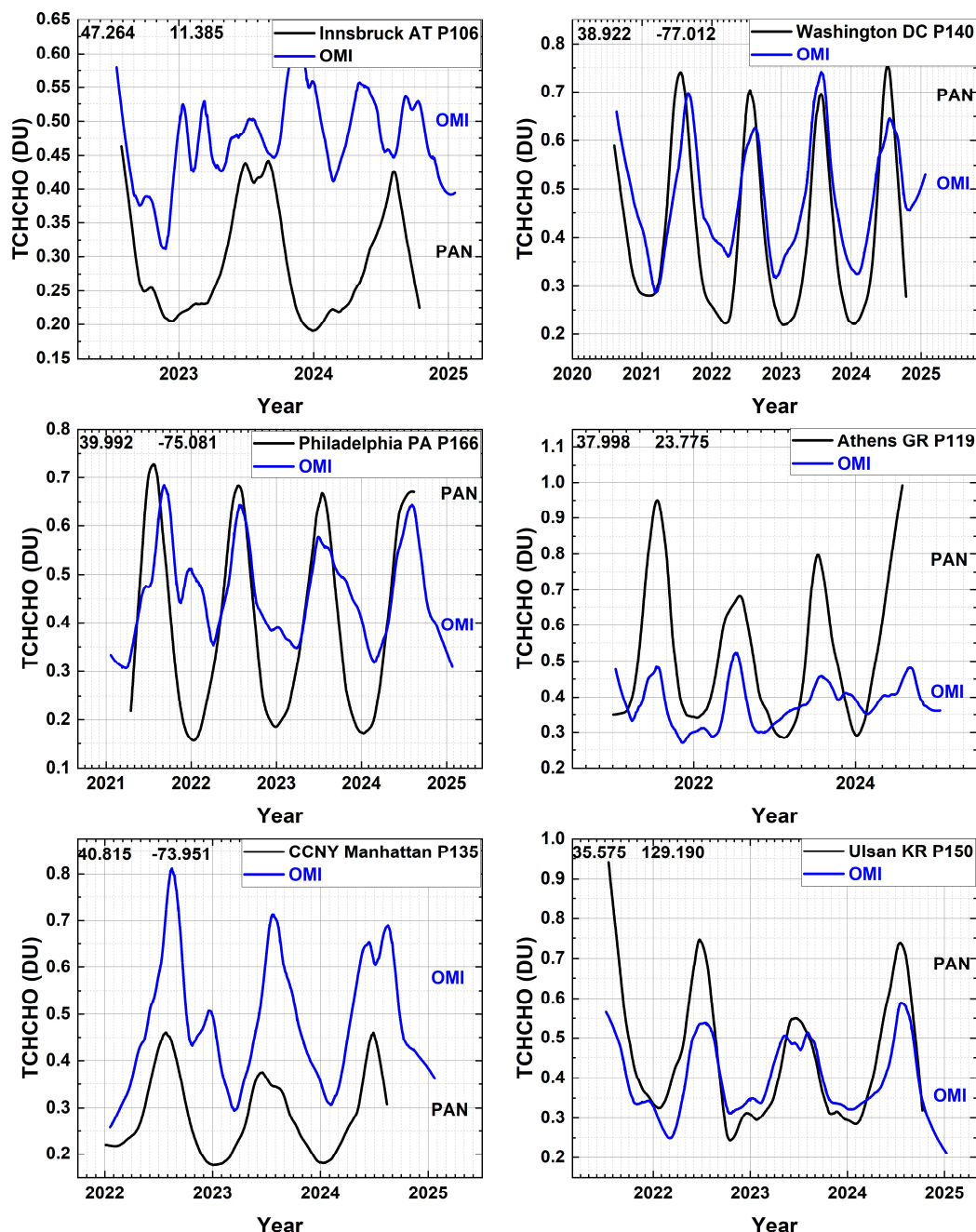


Figure A2 Six cases from Fig. A1 that have significant seasonal variation in TCHCHO. The numbers in the upper left corner are the latitude and longitude in degrees and the Pandora instrument number in the right corner. Principal Investigators are: P106 Dr. Martin Tiefengraber, P140 Dr. Jim Szykman, P166 Dr. Lucas Valin, P119 Dr. Stelios Kazadsi, P135, Dr. Maria Tzortziou, and P150 Dr. Chang Keun Song.

343
 344 Figure A2 shows additional cases where OMI and Pandora see the same seasonal dependence but differ
 345 on the amount of TCHCHO retrieved.

4.0 References

- Boeke NL, Marshall JD, Alvarez S, Chance KV, Fried A, Kurosu TP, Rappenglück B, Richter D, Walega J, Weibring P, Millet DB. Formaldehyde columns from the Ozone Monitoring Instrument: Urban versus background levels and evaluation using aircraft data and a global model, *J. Geophys. Res.* 2011 Mar 16;116(D5):10.1029/2010jd014870, doi: 10.1029/2010jd014870, 2011.
- Boersma, Klaas & Jacob, D. & Trainic, Miri & Rudich, Yinon & De Smedt, Isabelle & R, Dirksen & Eskes, Henk, Validation of urban NO₂ concentrations and their diurnal and seasonal variations observed from space (SCIAMACHY and OMI sensors) using in situ measurements in Israeli cities. *Atmos Chem Phys*, 9. 10.5194/acp-9-3867-2009, 2009.
- Cleveland, W. S.: Robust Locally Weighted Regression and Smoothing Scatterplots, *J. Am. Stat. Assoc.*, 74, 829–836, <https://doi.org/10.2307/2286407>, 1979.
- Cleveland, W. S. and Devlin, S. J.: Locally Weighted Regression: An Approach to Regression Analysis by Local Fitting, *J. Am. Stat. Assoc.*, 83, 596–610, <https://doi.org/10.1080/01621459.1988.10478639>, 1988.
- Faustini, Annunziata and Rapp, Regula and Forastiere, Francesco, Nitrogen dioxide and mortality: review and meta-analysis of long-term studies, *European Respiratory Journal*, 44, 744–753, <https://doi.org/10.1183/09031936.00114713>, 2014.
- Gratien, A., B. Picquet-Varrault, J. Orphal, E. Perraudin, J.-F. Doussin and J.-M. Flaud, Laboratory intercomparison of the formaldehyde absorption cross sections in the infrared (1660–1820 cm⁻¹ and ultraviolet (300–360 nm) spectral regions, *J. Geophys. Res.*, **112**, <https://doi.org/10.1029/2006JD007201>, D05305 1–10, 2007.
- Herman, J., A. Cede, E. Spinei, G. Mount, M. Tzortziou, and N. Abuhassan, NO₂ column amounts from ground-based Pandora and MFDOAS spectrometers using the direct-sun DOAS technique: Intercomparisons and application to OMI validation, *J. Geophys. Res.*, 114, D13307, doi:[10.1029/2009JD011848](https://doi.org/10.1029/2009JD011848), 2009.
- Herman, J., Huang, L., McPeters, R., Ziemke, J., Cede, A., and Blank, K.: Synoptic ozone, cloud reflectivity, and erythemal irradiance from sunrise to sunset for the whole earth as viewed by the DSCOVR spacecraft from the earth sun Lagrange 1 orbit, *Atmos. Meas. Tech.*, 11, 177–194, <https://doi.org/10.5194/amt-11-177-2018>, 2018.
- Herman, J., Abuhassan, N., Kim, J., Kim, J., Dubey, M., Raponi, M., and Tzortziou, M.: Underestimation of column NO₂ amounts from the OMI satellite compared to diurnally varying ground-based retrievals from multiple PANDORA spectrometer instruments, *Atmos. Meas. Tech.*, 12, 5593–5612, <https://doi.org/10.5194/amt-12-5593-2019>, 2019.
- Kim, K. H., Jahan, S. A., & Lee, J. T., Exposure to Formaldehyde and Its Potential Human Health Hazards. *Journal of Environmental Science and Health, Part C*, 29(4), 277–299. <https://doi.org/10.1080/10590501.2011.629972>, 2011.

- 391 Lamsal, L. N., Krotkov, N. A., Celarier, E. A., Swartz, W. H., Pickering, K. E., Bucsela, E. J., Gleason, J. F.,
 392 Martin, R. V., Philip, S., Irie, H., Cede, A., Herman, J., Weinheimer, A., Szykman, J. J., and Knepp, T. N.:
 393 Evaluation of OMI operational standard NO₂ column retrievals using in situ and surface-based NO₂
 394 observations, *Atmos. Chem. Phys.*, 14, 11587–11609, <https://doi.org/10.5194/acp-14-11587-2014>,
 395 2014.
- 396
 397 Lamsal, L., Duncan, Bryan, Yoshida, Yasuko, Krotkov, Nickolay, Pickering, Kenneth, Streets, David, Lu,
 398 Zifeng, U.S. NO₂ trends (2005–2013): EPA Air Quality System (AQS) data versus improved observations
 399 from the Ozone Monitoring Instrument (OMI). *Atmospheric Environment*. 110.
 400 10.1016/j.atmosenv.2015.03.055, 2015.
- 401
 402 Levelt, P. F., Joiner, J., Tamminen, J., Veefkind, J. P., Bhartia, P. K., Stein Zweers, D. C., Duncan, B. N.,
 403 Streets, D. G., Eskes, H., van der A, R., McLinden, C., Fioletov, V., Carn, S., de Laat, J., DeLand, M.,
 404 Marchenko, S., McPeters, R., Ziemke, J., Fu, D., Liu, X., Pickering, K., Apituley, A., González Abad, G.,
 405 Arola, A., Boersma, F., Chan Miller, C., Chance, K., de Graaf, M., Hakkarainen, J., Hassinen, S., Ialongo, I.,
 406 Kleipool, Q., Krotkov, N., Li, C., Lamsal, L., Newman, P., Nowlan, C., Suleiman, R., Tilstra, L. G., Torres, O.,
 407 Wang, H., and Wargan, K.: The Ozone Monitoring Instrument: overview of 14 years in space, *Atmos.*
 408 *Chem. Phys.*, 18, 5699–5745, <https://doi.org/10.5194/acp-18-5699-2018>, 2018.
- 409 Morfopoulos C, Müller J-F, Stavrakou T, et al. Vegetation responses to climate extremes recorded by
 410 remotely sensed atmospheric formaldehyde. *Glob Change Biol.*, 28, 1809–1822.
 411 <https://doi.org/10.1111/gcb.15880>, 2021.
- 412
 413 Newmark, G. (2001). Emissions Inventory Analysis of Mobile Source Air Pollution In Tel Aviv, Israel,
 414 *Transportation Research Record*, Vol. 1750, p. 40-48, <https://doi.org/10.3141/1750-0>, 2001.
- 415
 416 Nussbaumer, C. M., Crowley, J. N., Schuladen, J., Williams, J., Hafermann, S., Reiffs, A., Axinte, R.,
 417 Harder, H., Ernest, C., Novelli, A., Sala, K., Martinez, M., Mallik, C., Tomsche, L., Plass-Dülmer, C., Bohn,
 418 B., Lelieveld, J., and Fischer, H.: Measurement report: Photochemical production and loss rates of
 419 formaldehyde and ozone across Europe, *Atmos. Chem. Phys.*, 21, 18413–18432,
<https://doi.org/10.5194/acp-21-18413-2021>, 2021.
- 420
 421 Peng, W.-X., X.-C. Yue, H.-L. Chen, N.L. Ma, Z. Quan, Q. Yu, C. Sonne, A review of plants formaldehyde
 422 metabolism: Implications for hazardous emissions and phytoremediation, *J. Hazard. Mater.* 436 Article
 129304, <https://doi.org/10.1016/j.jhazmat.2022.129304>, 2022.
- 423
 424 Spinei, E., Whitehill, A., Fried, A., Tiefengraber, M., Knepp, T. N., Herndon, S., Herman, J. R., Müller, M.,
 425 Abuhassan, N., Cede, A., Richter, D., Walega, J., Crawford, J., Szykman, J., Valin, L., Williams, D. J., Long,
 426 R., Swap, R. J., Lee, Y., Nowak, N., and Poche, B.: The first evaluation of formaldehyde column
 427 observations by improved Pandora spectrometers during the KORUS-AQ field study, *Atmos. Meas. Tech.*,
 11, 4943–4961, <https://doi.org/10.5194/amt-11-4943-2018>, 2018.
- 428
 429 Spinei, E., Tiefengraber, M., Müller, M., Gebetsberger, M., Cede, A., Valin, L., Szykman, J., Whitehill, A.,
 430 Kotsakis, A., Santos, F., Abuhassan, N., Zhao, X., Fioletov, V., Lee, S. C., and Swap, R.: Effect of
 431 polyoxymethylene (POM-H Delrin) off-gassing within the Pandora head sensor on direct-sun and multi-
 432 axis formaldehyde column measurements in 2016–2019, *Atmos. Meas. Tech.*, 14, 647–663,
<https://doi.org/10.5194/amt-14-647-2021>, 2021.

- 433 Stavrakou, T., Müller, J.-F., Bauwens, M., Boersma, K. F. & van Geffen, J. Satellite evidence for changes in
 434 the NO₂ weekly cycle over large cities. *Sci. Rep.* <https://doi.org/10.1038/s41598-020-66891-0> (2020).
- 435 Tzortziou, M., Herman, J.R., Cede, A. *et al.* Spatial and temporal variability of ozone and nitrogen dioxide
 436 over a major urban estuarine ecosystem. *J Atmos Chem* **72**, 287–309, [https://doi.org/10.1007/s10874-](https://doi.org/10.1007/s10874-013-9255-8)
 437 [013-9255-8](https://doi.org/10.1007/s10874-013-9255-8), 2015.
- 438 Van der A, R. J., H. J. Eskes, K. F. Boersma, T. P. C. van Noije, M. Van Roozendaal, I. De Smedt, D. H. M. U.
 439 Peters, and E. W. Meijer, Trends, seasonal variability and dominant NO_x source derived from a ten year
 440 record of NO₂ measured from space, *J. Geophys. Res.*, 113, D04302, doi:10.1029/2007JD009021, 2008.
- 441 Wang, P.; Holloway, T.; Bindl, M.; Harkey, M.; De Smedt, I. Ambient Formaldehyde over the United
 442 States from Ground-Based (AQS) and Satellite (OMI) Observations. *Remote Sens.* 14, 2191,
 443 <https://doi.org/10.3390/rs14092191>, 2022.
- 444 Wittrock, F., Richter, A., Oetjen, H., Burrows, Wittrock, F., Richter, A., Oetjen, H., Burrows, J.P., Kanakidou,
 445 Myriokefalitakis, S., Volkamer, R., Beirle, S., Platt, U., and Wagner, T.: Simultaneous global observations of
 446 glyoxal and formaldehyde from space, *Geophys. Res. Lett.*, 33, L16804,
 447 <https://doi.org/10.1029/2006GL026310>, 2006.
- 448 Zhang, Y., Li, R., Min, Q., Bo, H., Fu, Y., Wang, Y., & Gao, Z. (2019). The controlling factors of atmospheric
 449 formaldehyde (HCHO) in Amazon as seen from satellite. *Earth and Space Science*, 6, 959–971.
 450 <https://doi.org/10.1029/2019EA000627>, 2019.

451

Author contribution:

Jay Herman is responsible for writing the paper and creating the figures. Jianping Mao obtained the EPIC overpass data for the Pandora sites and discussed aspects of the paper.

Data Availability

Worldwide Pandora data for 63 sites is available from the Austrian Pandonia project website <https://data.pandonia-global-network.org/> or from a NASA backup site updated every week.

https://avdc.gsfc.nasa.gov/pub/DSCOV/Pandora/DATA_02/

The OMI overpass TCHCHO and TCNO2 data are found at

<https://avdc.gsfc.nasa.gov/pub/data/satellite/Aura/OMI/V03/L2OVP/OMHCHO/>.

<https://avdc.gsfc.nasa.gov/pub/data/satellite/Aura/OMI/V03/L2OVP/OMNO2/>

OMI TCO overpass data are available from

<https://avdc.gsfc.nasa.gov/pub/data/satellite/Aura/OMI/V03/L2OVP/OMTO3/>

Competing interests:

The authors declares that they have no conflicts of interest.

Funding: This study is funded by the DSCOV-EPIC project through the University Of Maryland Baltimore County

Acknowledgements:

The authors want to acknowledge the contribution of each of the Pandora Principal Investigators included in the figure captions and for the OMI team and Dr. Lok Lamsal for making OMI overpass data available. Acknowledgement is also due to the Pandonia team lead by Dr. Alexander Cede for processing all of the Pandora data and devising the retrieval algorithms and to Dr. Nader Abuhassan for building and calibrating all of the Pandora spectrometer systems. The Pandonia Global Network PGN is a bilateral project supported with funding from NASA and ESA.

479 Figure Captions

480 Fig. 1 Seasonal and daily behavior of HCHO and NO₂ from Pan 180 located in the Bronx, NYC at 40.868°N,
481 -73.878°W. The blue lines are a Lowess(0.033) fit to the data (light grey), which is approximately a 1-
482 month local least-squares average. The Local principal investigator for Pan 180 is Dr. Luke Valin.

483 Fig. 2 The daily average seasonal variation of HCHO and NO₂ over Fordham University in Bronx, New
484 York City from Pandora 180 at 40.868° latitude, -73.878° longitude, and 0.003 km altitude. Each point is
485 a daily average of the data in Fig.1. Local principal investigator: Dr. Luke Valin

486 Fig. 3 The seasonal variation of TCHCHO and TCNO₂ over New Haven Connecticut from Pandora 64 at
487 41.301°N latitude and -72.903°W longitude. Each point is a daily average. Local principal investigator:
488 Dr. Nader Abuhassan.

489 Fig. 4 The seasonal variation of TCHCHO and TCNO₂ over equatorial Bangkok Indonesia at 13.785°N and
490 100.540°E. The local principal investigator is Surassawadee Phoompanit.

491 Fig. 5 Seasonal variation in daily average TCHCHO and TCNO₂ in Tel Aviv Israel from Pandora 182 located
492 at 32.113°N 34.085°E at a height of 8 meters. The local principal investigator for Pan 182 is Dr. Michal
493 Rozenhaimer.

494 Fig. 6 Seasonal variation in daily average HCHO and NO₂ in Wakkerstroom South Africa from Pandora
495 159 located at -27.359°S and 30.144°E. Local principal investigator: B. Scholes

496 Fig. 7 Upper 2 Panels: Comparison of OMI (approximately 13:30) and Pandora (07:00 – 17:00) total
497 column NO₂ time series in Bronx NY (40.868°N, -73.878°W) and Busan Korea (35.235°N, 129.083°E).
498 Lower 4 Panels: Pandora data for Bronx, Busan, Philadelphia (39.992°N, -75.081°W) and Boulder
499 (40.0375°N, -105.242°W) are averaged between 13:00 – 14:00 hours. Both OMI (blue) and Pandora
500 (black) then have a Lowess(3-month) low-pass filter applied. Local principal investigator for Pan20 is Jae
501 Hwan Kim, for Pan 180 and Pan 166 is Dr. Luke Valin, and for Pan 204 Dr. Nader Abuhassan.

502 Fig. 8 A comparison between Pandora and OMI (Orange circle) total column NO₂ for 3 locations (Bronx,
503 New York, Busan Korea, Philadelphia, Pennsylvania. The Local principal investigator for Pan 180 and Pan
504 166 is Dr. Lukas Valin and for Pan 20 is Dr. Jae Hwan Kim.

505 Fig. 9 A comparison between Pandora and OMI (purple circle) total column HCHO. The Local principal
506 investigator for Pan 180 is Dr. Luke Valin and for Pan 20 is Dr. Jae Hwan Kim.

507 Fig. 10 A comparison of Pandora TCHCHO and TCNO₂ daily average total column amounts for Toronto-
508 Scarborough University of Toronto and OMI data for Toronto East (43.740°N, -79.270°W at
509 approximately 13:20±0:20 Local Sun Time, GMT + Longitude/15). The local principal investigator for Pan
510 145 is Dr. Vitali Fioletov.

511 Fig. 11 TCNO₂ annual cycle for Toronto Scarborough from Pan 145 average between 13:00 and 14:00
512 and OMI. The smooth curves are Lowess(6 Months).

Fig. 12 A comparison between low-pass filtered, Lowess(3 months), OMI and Pandora at six sites with

varying degrees of agreement with $TCHCHO(Pan) < TCHCHO(OMI)$. The Local Principal Investigators are P106 Dr. Stefano Casadio, Dr. Kei Shiomi P193, Dr. Alexander Cede P204, Dr. Lukas Valin P39; P134, and Dr. Martin Tiefengraber P106. Latitudes and longitudes are in each upper left corner.

Fig. 13 A comparison of OMI Total Column Ozone values with those obtained from Pandora 140 over the Washington DC site at $38.922^{\circ}N$ and $-77.012^{\circ}W$ and with those obtained from Pandora 20 over the Busan, Korea site at $32.325^{\circ}N$ and $129.083^{\circ}E$. The smooth curves (right panel) are Lowess(6-month) fits to data in the left panel. The local principal investigator for Pan 140 is Dr. Jim Szykman and for Pan20 is Jae Hwan Kim.

Fig. 14 A comparison of Pandora and OMI retrievals of total column O_3 at the time of the OMI satellite overpass. Local Principal Investigators: Pan 240 Alexander Cede, Pan 238 Inmaculada Foyo Moreno, Pan 166 Lukas Valin, and Pan 190 Surassawadee Phoompan.

Fig. 15 A comparison of Pandora (Open Circles), EPIC (magenta stars), and OMI (orange circles) retrievals of total column O_3 at the times of the satellite overpasses. Local Principal Investigators: Pan 145 Vitali Fioletov, Pan 66 Lukas Valin, Pan 39 Lukas Valin, Pan 156 Alexander Cede, Pan 66 Nader Abuhassan, Pan180 Lukas Valin, and Pan 140 Jim Szykman.

Fig. A1 The seasonal cycle of TCHCHO in DU from 20 randomly selected Pandora TCHCHO time series. The numbers in the upper left corner are the latitude and longitude in degrees and the Pandora instrument number in the right corner.

Figure A2 shows additional cases where OMI and Pandora see the same seasonal dependence but differ on the amount of TCHCHO retrieved.